Life Cycles of Blocking Flows Associated with Synoptic-Scale Eddies: Observed Results and Numerical Experiments

Luo Dehai (罗德海)①

Department of Atmospheric and Oceanic Sciences, Oceanic University of Qingdao, LASG, Institute of Atmospheric Physics, Chinese Academy of Sciences, Beijing 100029

Li Jianping (李建平)

LASG, Institute of Atmospheric Physics, Chinese Academy of Sciences, Beijing 100029

Huang Fei (黄 菲)

Department of Atmospheric and Oceanic Sciences, Ocean University of Qingdao, Qingdao, 266003

(Received July 15, 2001; revised March 20, 2002)

ABSTRACT

An observational study is presented to confirm that the life cycle of blocking associated with synoptic-scale eddies is a transfer process between dispersion and nondispersion. In addition, numerical experiments are conducted. It is found that the synoptic-scale eddies seem to play a dominant role in the amplification of blocking, while the topography effect appears to play a phase-locking role. At the same time, the synoptic eddies tend to split into two branches during the onset of blocking. This supports the observational results obtained.

Kery words: blocking, life cycle, synoptic-scale eddy

1. Introduction

Over the past several decades, many theoretical studies have been made to model atmospheric blockings that can persist for times of about 10 or more days (Yeh 1949; Egger 1978; Charney and DeVore 1979; McWilliams 1980; Malguzzi and Malanotte-Rizzoli 1984; Haines and Marshall 1987; Malguzzi 1993). However, no complete theory has been realistically proposed to model the life cycle of blocking associated with synoptic-scale eddies so far. Observational and numerical studies have confirmed that the onset, maintenance and decay of blocking circulations are strongly associated with transient baroclinic disturbances (Berggren et al. 1949; Green 1977; Hansen and Chen 1982; Reinhold and Pierrehumbert 1982; Illari and Marshall 1983, Illari 1984; Shutts 1983, 1986; Ji and Tibladi 1983; Egger et al. 1986; Metz 1986; Mullen 1987; Holopainen and Fortelius 1987; Colucci 1985, 1987; Vautard et al. 1988; Vautard and Legras 1988; Nakamura and Wallace 1990, 1993; Nakamura et al. 1997; Tsou and Smith 1990; Tanaka 1991; Chen and Juang 1992; Lupo and Smith 1995). Recently, Nakamura et al. (1997) showed that the transient eddy feedback from the synoptic-scale migratory eddies can account for more than 75% of the observed amplification of the Pacific blocking and less than 45% for the European block. In the last two decades, the modon and

①E-mail: ldh@ouqd.edu.cn

soliton were thought of as being two models applicable to describe observed blocking configurations (McWilliams 1980; Malguzzi and Malanotte–Rizzoli 1984; Malanotte–Rizzoli and Malguzzi 1987; Haines and Marshall 1987). Although the two kinds of theories have gained some success in explaining the horizontal structures and main characteristics of time–mean blockings, there is still a great discrepancy between theoretical and observed blockings for many aspects during their life cycles. In particular, the life cycle of blocking by synoptic–scale eddies and its physical mechanism cannot be described better. This motivates us to seek a new theory to describe the life cycle of blocking associated with synoptic–scale eddies (Luo 1999, 2000).

More recently, in a two–layer model, Luo (2000) studied the dynamics of a transient–forced envelope Rossby soliton and attempted to apply it to the explanation of the life cycle of blocking attributed to the nonlinear, upscale energy transfer from synoptic–scale eddies. Based on his theory, how a planetary–scale blocking wave changes during the interaction with synoptic–scale disturbances and how the synoptic–scale waves are modulated by the amplified blocking can be clearly understood. He further found that the establishment of blocking by synoptic–scale eddies is a transfer of an amplifying envelope soliton from dispersion to weak dispersion (even non–dispersion), while there is a reverse process during the decay stage of blocking. However, no observational evidence is presented to confirm the theoretical results. Therefore, it is necessary for us to make a quantitative evaluation of the relevance of the transient forced envelope Rossby soliton to observed blocking using observational data. In addition, numerical experiments are presented to distinguish the different roles of synoptic–scale eddies and wavenumber–two topography in producing blocking.

The plan of this paper is as follows. In section 2 we present the observational evidence of a transfer of a blocking system between dispersion and weak dispersion (even non–dispersion). A numerical experiment on the life cycle of blocking associated with synoptic–scale eddies over a wavenumber–two topography is presented in section 3 in order to discern the different roles of synoptic eddies and wavenumber–two topography in producing blocking. Conclusions are presented in section 4.

2. Data analysis and the transfer of a blocking system between dispersion and weak dispersion (even non–dispersion)

In this section, an observational study is carried out to seek confirmation of the proposed forced theory (Luo 1999, 2000; Luo and Li 2000). The data used in this investigation consist of 500 hPa geopotential height data of the NCEP/NCAR reanalysis on a 2.5° × 2.5° latitude–longitude grid. The full grid extends from 30°N to 80°N and westward from 40°W to 120°E.

Here the geostrophic streamfunction was calculated at each grid point (i, j) as $\psi_{i,j} = f_0^{-1} g Z_{i,j}$, where f_0 is the Coriolis parameter at 60°N, g is the gravitational acceleration, and $Z_{i,j}$ is the geopotential height of the isobaric surface. Figure 1 shows the geostrophic streamfunction fields at each day (1200 UTC) during the life cycle of blockings from 1 to 22 February 1989.

As shown in Fig. 1a, from 1 to 14 February a blocking event occurred over the North Pacific Ocean, but from the 14 to 22 February another blocking event occurred over the same

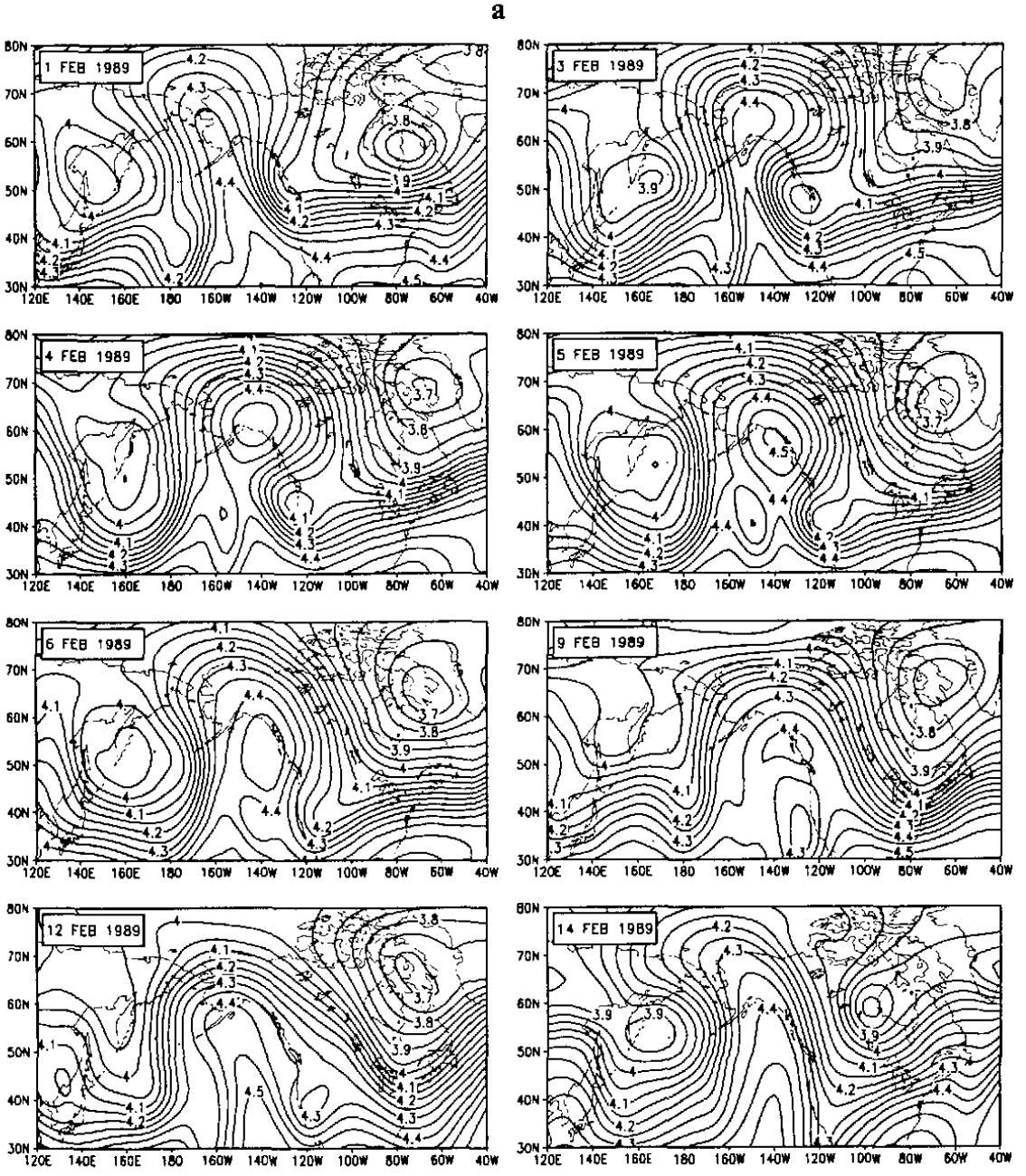

Fig. 1. The 500 hPa geostrophic streamfunction ψ of blocking events formed over the North Pacific Ocean during the period from 1 to 22 February 1989. (a) Total field, contour interval (CI) is 5×10^6 m^2 s^{-1}; (b) planetary–scale field, CI $= 5 \times 10^6$ m^2 s^{-1}; (c) synoptic–scale field, CI $= 2 \times 10^6$ m^2 s^{-1}.

region. It is easy to find that the blocking region is occupied by several cyclonic eddies during the life cycle of each blocking. Therefore, it can be concluded through a comparison with Luo (1999, 2000) that the block circulation in Fig. 1a is excited by the synoptic–scale eddies upstream, which is similar to the blocking pattern first found by Berggren et al. (1949). Correspondingly, Fig. 1b is the planetary–scale field, defined as the sum of harmonic

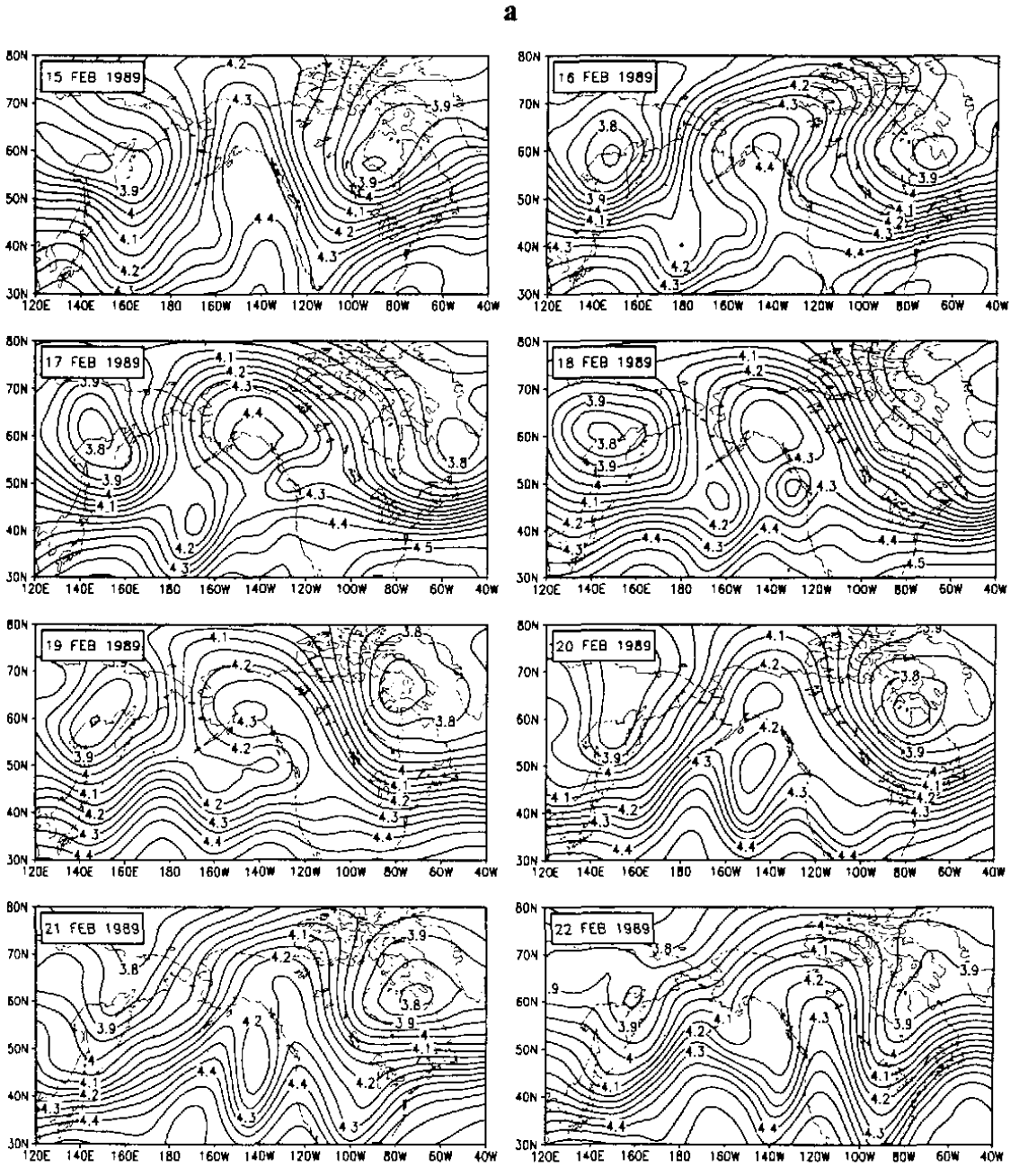

Fig. 1. (Continued).

components with zonal wavenumbers 0–3, while Fig. 1c is the synoptic–scale field between zonal wavenumbers 7 and 25. At 1 February 1989, a weak blocking ridge (an incipient block) appeared, which is seen as a planetary–scale ridge prior to block onset. Due to the deepening of upstream synoptic–scale eddies, this blocking ridge enhances and evolves into an asymmetric dipole block. At the same time, the synoptic–scale eddies seem to be enhanced and split into two branches before the typical blocking is established. This splitting is particularly noticeable over the upstream and downstream flanks of the blocking region. However,

b

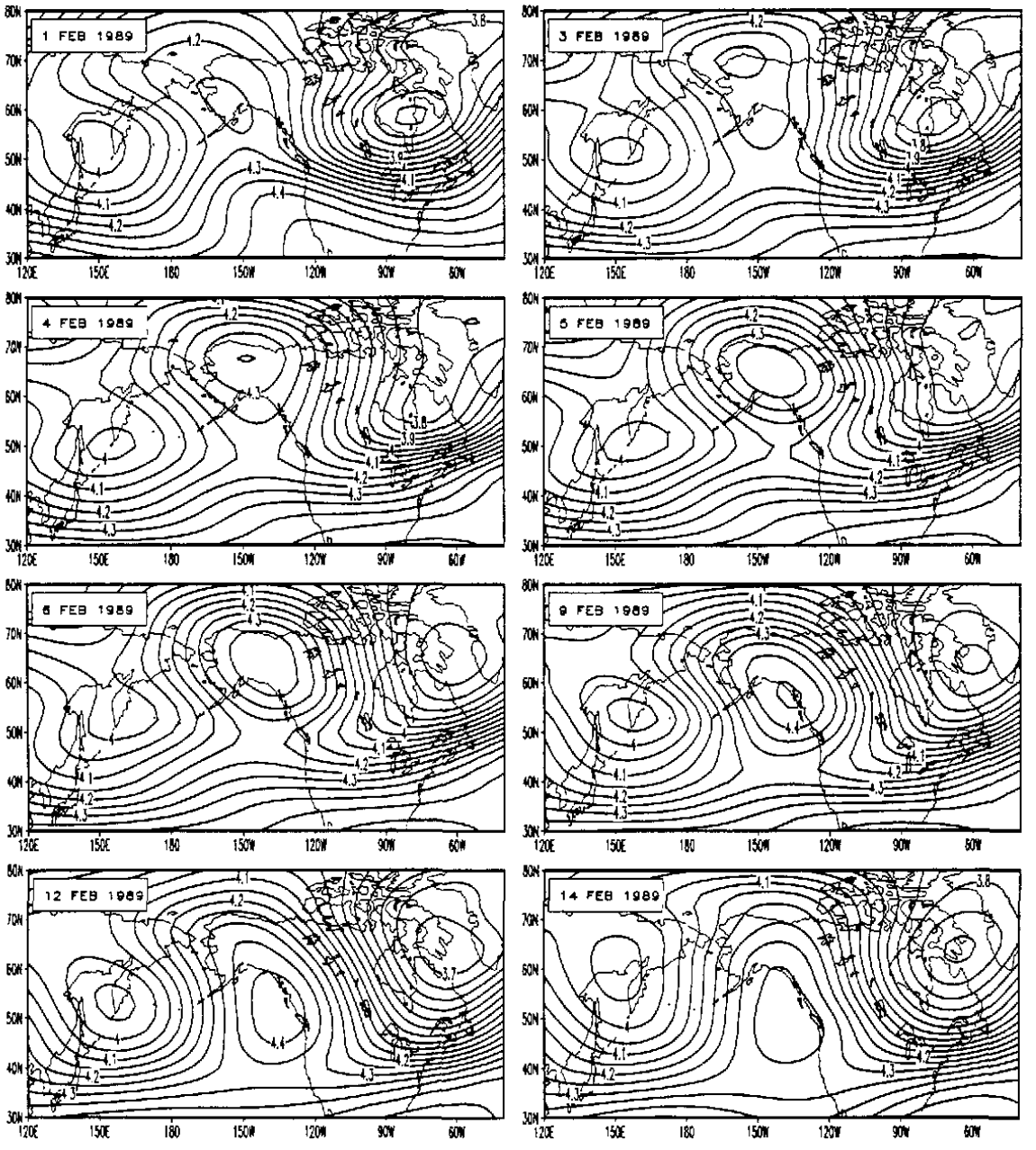

Fig. 1. (Continued).

during the period of blocking decay (9–14 February 1989), the synoptic–scale eddies also weaken. This interaction between blocking wave and synoptic–scale eddies is easily explained in terms of theory (Luo 1999, 2000; Luo and Li 2000; Luo et al. 2001). After 14 February 1989, a new blocking cycle begins. In this blocking event, the drastic change of the synoptic–scale eddies cannot be seen, but the splitting of the synoptic eddies can still be observed. Furthermore, its planetary–scale field exhibits an omega–type blocking high. Thus, we conclude that in the second blocking cycle, the topography effect seems to become

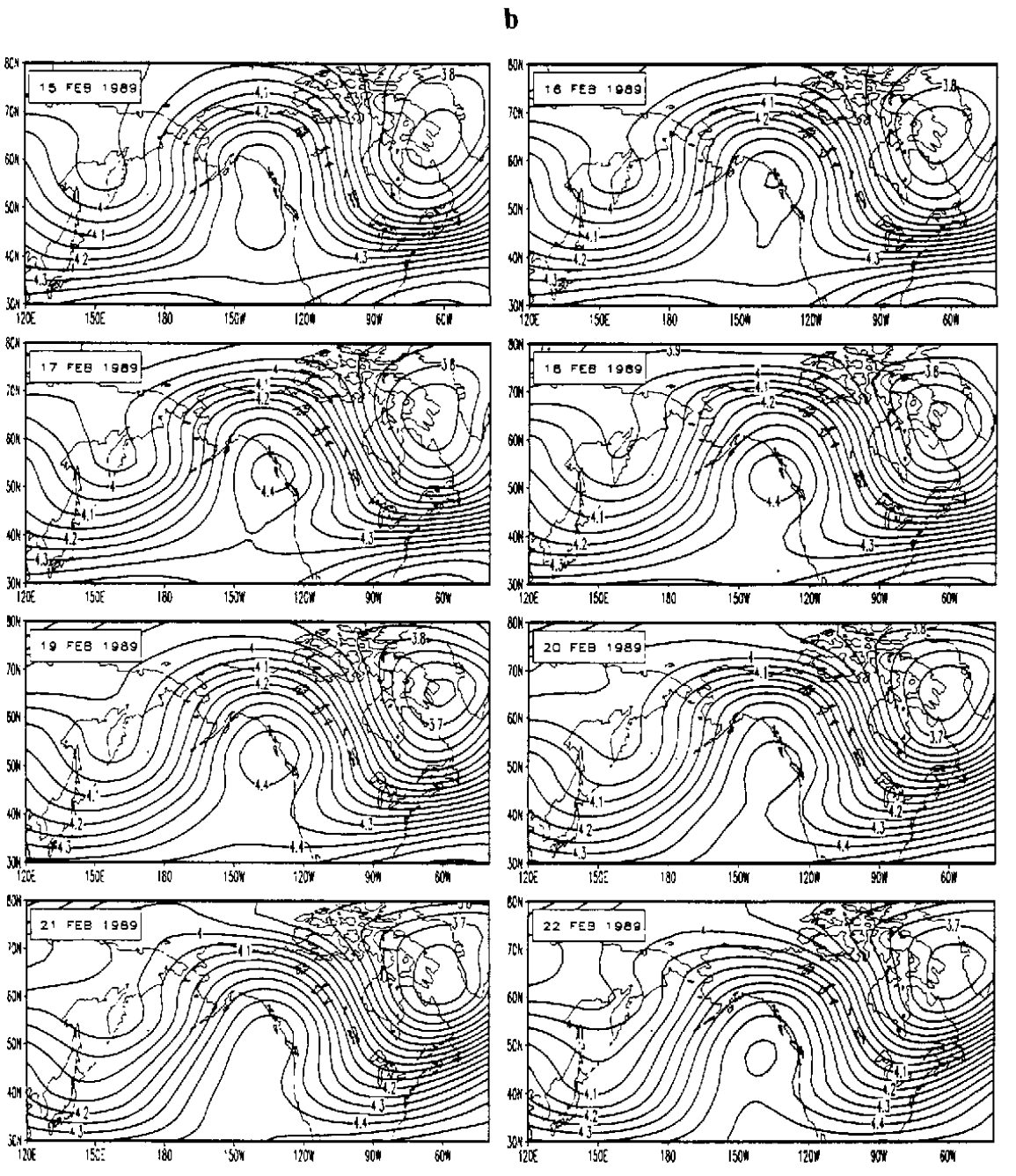

Fig. 1. (Continued).

dominant. This is because the dominant blocking high having a monopole meridional structure seems to be induced by the topography with the same meridional structure.

Although the studies presented by Luo (1999, 2000) and Luo and Li (2000) can provide a possible explanation for the establishment, maintenance and decay of blocking by synoptic–scale eddies, an important question remains unsolved. That is, we wish to determine whether the evolution of the amplitude, wavelength and the difference between group velocity and phase speed of observed blocking compares qualitatively with the observations. The issue

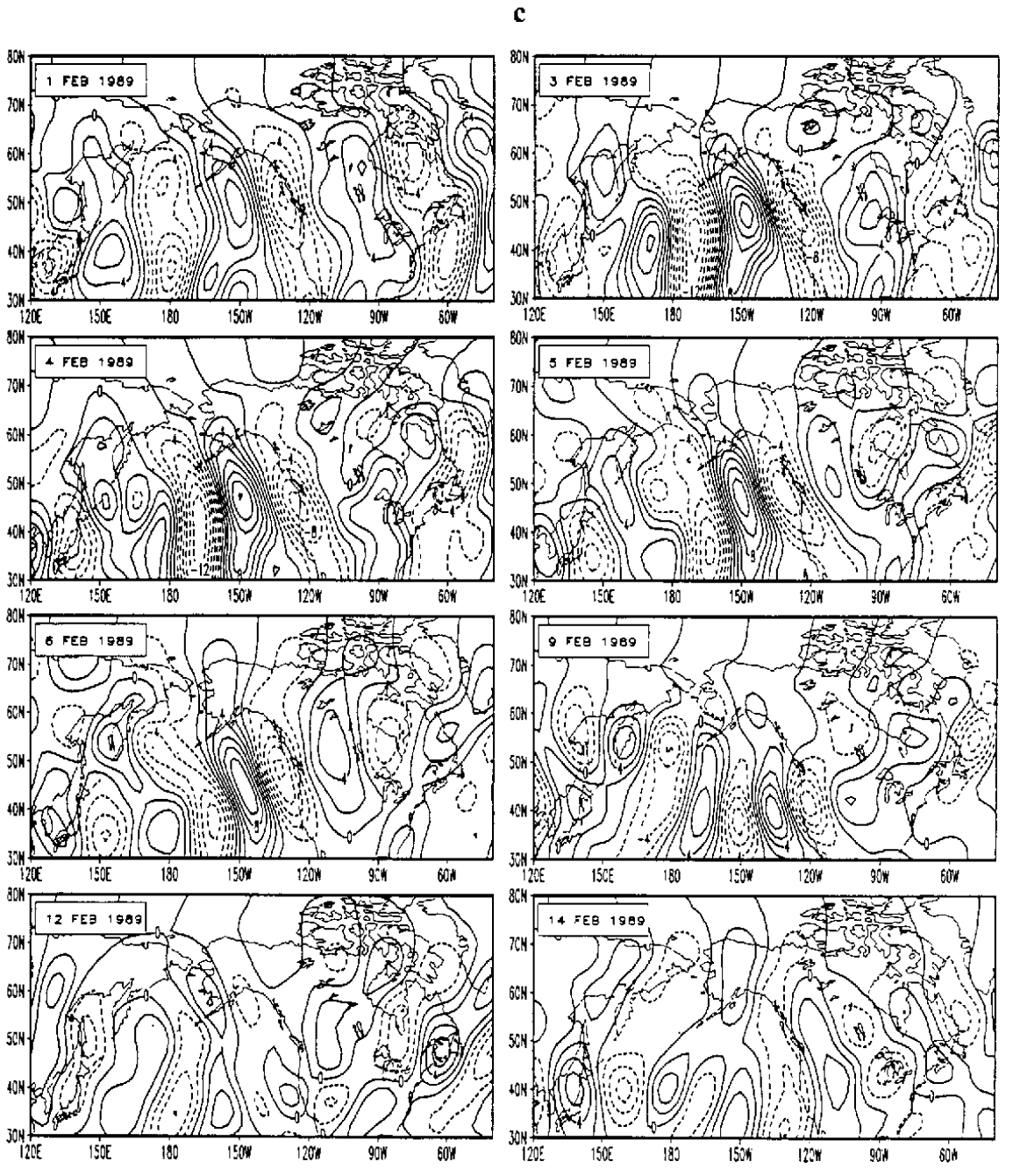

Fig. 1. (Continued).

will be further expounded here.

In this section, to approximately obtain the time evolution of the amplitude, wavelength and the difference between group velocity and phase speed of blocking wave during the life cycle of blocking, the shorter waves for zonal wavenumbers greater than 5 were filtered out. In the present study, the mean value of the closed high pressure center in the blocking high region may be crudely regarded as the amplitude of blocking. For the blocking cases discussed here, the closed center of the blocking high lies mainly between 50°N and 70°N. If Z_p is

c

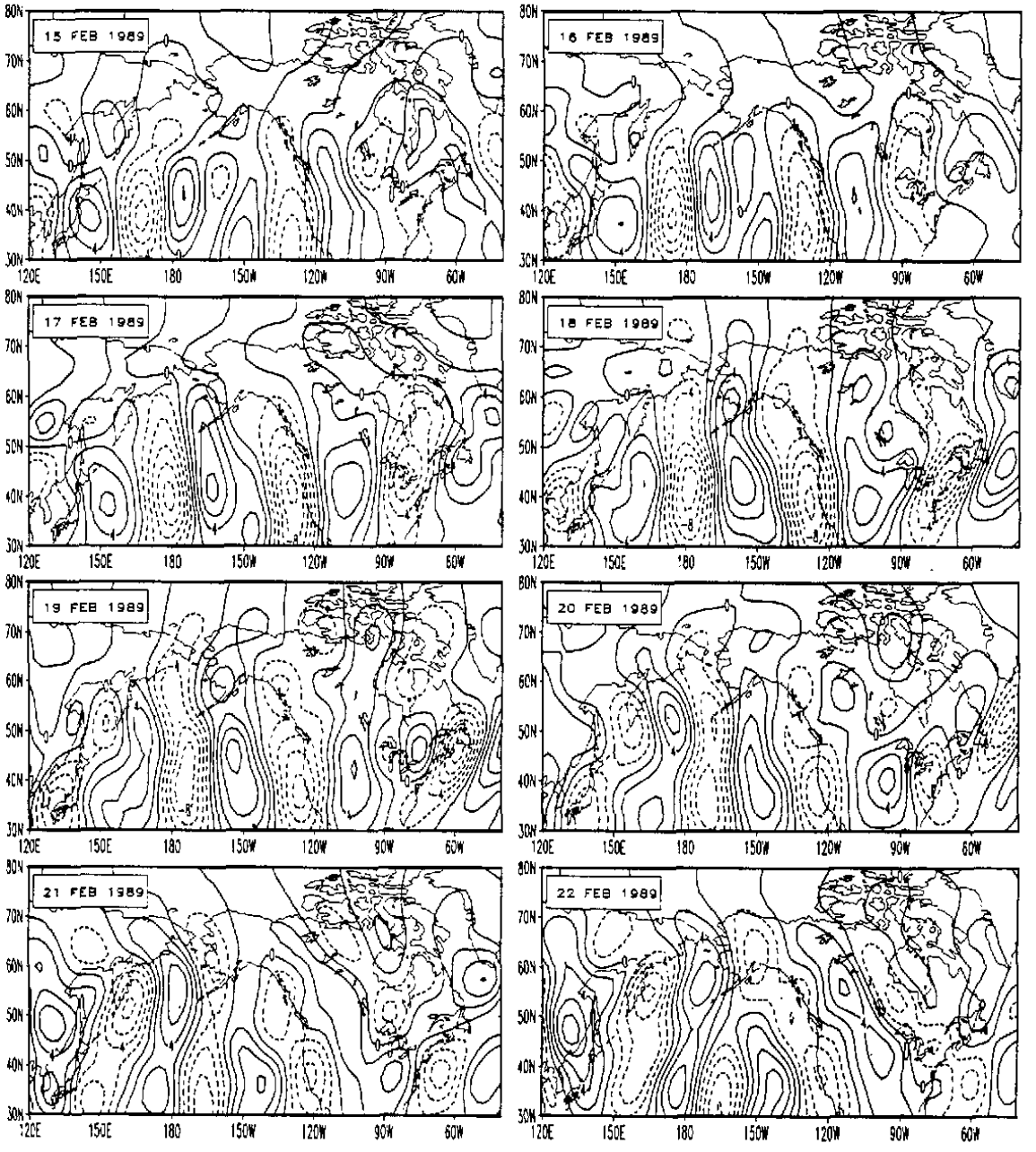

Fig. 1. (Continued).

defined as the planetary–scale part of observed blocking, then it is convenient to define

$$A(\lambda, t)= \frac{1}{\varphi_2 - \varphi_1}\int_{\varphi_1}^{\varphi_2} Z_p(\lambda, \varphi, t)d\varphi \ , \tag{1}$$

where λ, φ and t are the longitude, latitude and time, respectively. Thus we may choose $\varphi_1 = 50°$N and $\varphi_2 = 70°$N. The mean value, $M(t)$, of $A(\lambda, t)$ in the region of the blocking high center can be obtained from (1). Further, we define $m(t)= \min[m_1(t), m_r(t)]$, where $m_1(t)$ and

$m_r(t)$ are the mean amplitudes of the low pressure centers over the two sides of the blocking high, left and right, respectively. In this case, the amplitude of the blocking high can be defined as

$$M_z(t)= [M(t)- m(t)+ \delta_y(t)]/2 , \tag{2}$$

where $\delta_y(t)$ is the difference between the mean geopotential heights in the closed center of the blocking high region, bounded by the latitudes 50°N and 70°N and longitudes 115°W and 195°W, and in the closed low pressure center over the south side of the blocking high, bounded by the latitudes 40°N and 50°N and longitudes 15°W and 95°W.

If the position of the blocking high center, denoted by $A(\lambda, t)$, is defined as $x_M(t)$, and the positions of the low pressure centers or troughs over its left and right sides are defined as $x_l(t)$ and $x_r(t)$, then the zonal wavelength of planetary–scale blocking can be approximated as

$$L_x(t)= \text{dist}[x_l(t), x_r(t)] . \tag{3}$$

It is difficult to exactly determine the group velocity and phase speed of the observed blocking system. However, we can approximately obtain the group velocity of the observed blocking system according to the energy dispersion principle which gives the group velocity as the moving speed of the maximum amplitude wave. Based on this point, the group velocity of the observed blocking system can be approximately represented by the moving speed of the center of the blocking high, and written as

$$C_g(t)= \frac{dx_M(t)}{dt} \approx \frac{x_M(t+\Delta t)- x_M(t)}{\Delta t} . \tag{4}$$

The most striking feature observed during the onset (decay) of blocking is the rapid weakening (strengthening) of the background westerly wind. Thus, the change of the basic westerly wind over the blocking region can basically represent the changing of the phase speed of the observed blocking configuration at each stage. An effective method is to determine the phase speed of the dominated planetary wave that can basically describe observed blocking system. If the phase speed of the dominated planetary wave can be obtained, the phase speed of the observed blocking can be determined approximately. Based on this idea, it is easy to determine the phase speed of the observed blocking using the long Rossby wave theory. In Fig. 1, zonal wavenumber 2 is a dominant wave (figures omitted). In applying the Rossby long wave theory, the basic westerly wind can be considered as a constant at each stage, but is time–dependent during the period of blocking. The formula for Rossby long waves is omitted here.

If $C(t)$ is defined as the phase speed of the observed blocking, then we can define

$$|C_{gp}(t)|= |C_g(t)- C(t)| , \tag{5}$$

as a measure of the maintenance of the blocking system.

If $|C_{gp}(t)|$ becomes smaller (even zero), then blocking system may reach a weak dispersive (even nondispersive) state. This case just corresponds to the enhancement and maintenance of the blocking system by synoptic–scale eddies upstream because the corresponding blocking also reaches the maximum amplitude in this stage. Using formulas (1)–(5), then the time evolution of the amplitude for $M_z(t)$ of blocking, the wavelength for $L_x(t)$, and $|C_{gp}(t)|$ can be obtained during the two blocking episodes, as shown in Fig. 2.

It is found from Fig. 2 that a blocking ridge is formed at day 1. The weak block increases

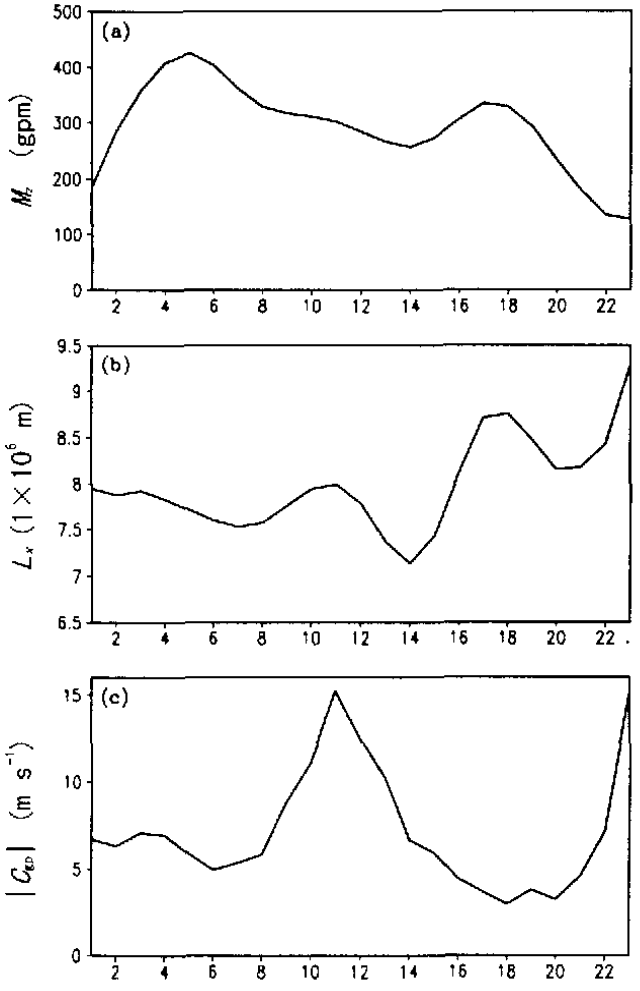

Fig. 2. Time evolution of $M_z(t)$, $L_x(t)$ and $|C_{gp}(t)|$ for blocking events occurring over the North Pacific Ocean during the period from 1 to 22 February 1989: (a) $M_Z(t)$; (b) $L_x(t)$; (c) $|C_{gp}(t)|$.

in amplitude and reaches its maximum amplitude by day 5 through the forcing of synoptic–scale eddies upstream. Afterwards, this block flow begins to decrease and reaches its minimum amplitude by day 14. During the period of days 3–6 a strong blocking circulation is established. Moreover, it can be noted that $|C_{gp}(t)|$ decreases (increases) during the onset (decay) stages of the block except for a small decreasing of blocking wavelength. During the second event of blocking (14–22 February), a significant change of $|C_{gp}(t)|$ and $L_x(t)$ is observed even though the changing of the blocking amplitude is not noticeable relative to the first blocking event. On the other hand, it is easily found that during the second blocking event, $|C_{gp}(t)|(L_x(t))$ decreases (increases) noticeably during the onset stage of the blocking, but during the decay stage of blocking both $|C_{gp}(t)|$ and $L_x(t)$ have a reverse change. These observational results confirm that the onset and maintenance of the blocking by synoptic–scale eddies is a transfer of the blocking system from strong dispersion to weak dispersion (even non–dispersion), while the decay of the blocking by synoptic–scale eddies has the reverse process. Thus, the transient forced dipole envelope soliton theory can, to some extent, explain the life cycle of the blocking by synoptic–scale eddies, however a large number of observational studies should be made to further verify the theory. On the other hand, it

should be pointed out that although the diagnostic study carried out here can provide some knowledge for understanding the role of the interaction between planetary waves and synoptic–scale eddies in the onset, maintenance and break–down of blocking, it cannot identify which scale eddies of synoptic–scale eddies more favor the establishment of blocking. This needs further study.

3. Numerical experiment on the life cycle of blocking associated with synoptic–scale eddies over a wavenumber–two topography

The purpose of this section is to study the different roles of synoptic–scale eddies and wavenumber–two topography in producing blocking.

A non–dimensional barotropic vorticity equation, as described in Luo (1999), is still used to model the life cycle of the blocking event in Fig. 1. Letting $\Psi_T = -\bar{u}y + \psi$, this non–dimensional vorticity equation can be written as

$$\left(\frac{\partial}{\partial t} + \bar{u}\frac{\partial}{\partial x}\right)(\nabla^2\psi - F\psi) + J(\psi, \nabla^2\psi + h) + (\beta + F\bar{u})\frac{\partial\psi}{\partial x} + \bar{u}\frac{\partial h}{\partial x} = 0 \ , \tag{6}$$

where $\bar{u}$ is a uniform basic flow that is required to sastify a stationary Rossby wave allowing $\bar{u} = \beta/(k^2 + m^2)$, and the other notation can be found in Luo (1999).

In Eq.(6), the Euler backward difference scheme is used to approximate the time differential and the Jacobian term is solved by the Arakawa space difference scheme, which assures the stability of numerical computation. The integration domain in this paper is $[-L_x/2 \leqslant x \leqslant L_x/2; 0 \leqslant y \leqslant L_y]$ for $L_x = 3L_y$ and $L_y = 5$. The space step chosen is $\Delta x = \Delta y = 0.125$ and the time step is $\Delta t = 0.024$. Note that there are solid boundary conditions over the northern and southern boundaries and periodic boundary conditions in the zonal direction.

For comparison, the wavy topography considered here is still a wavenumber–two topography. Then, we will study the response of a localized incipient blocking ridge to this wavy topography so as to further clarify the physical mechanism of the real blocking cycle. Similar to Charney and Devore (1979), the bottom topography is assumed to be a wavenumber–two topography of the form

$$h = 2h_0\cos(kx)\sin(my/2) \ , \tag{7}$$

where h_0 is the topographic amplitude, $k = 2/(6.371\cos\varphi_0)$ is the zonal wavenumber and $m = -2\pi/L_y$ is the meridional wavenumber.

The initial field here is chosen to consist of two parts: planetary–scale and synoptic–scale components, of the form

$$\psi = \psi_P + \psi_S \ , \tag{8}$$

and

$$\psi_P = 2\sqrt{\frac{2}{L_y}}M_0\,\mathrm{sech}\left[\sqrt{\frac{\delta}{2\lambda}}M_0 x\right]\cos(kx)\sin(my) + a\cos(kx)\sin(-my/2) \ , \tag{9a}$$

$$\psi_S = 2f_0[\cos(\tilde{k}_1 x) - \cos(\tilde{k}_2 x)]\sin(my/2) \ , \tag{9b}$$

$$f_0 = a_0\exp[-\gamma\varepsilon^2(x + x_0)^2] \ , \tag{9c}$$

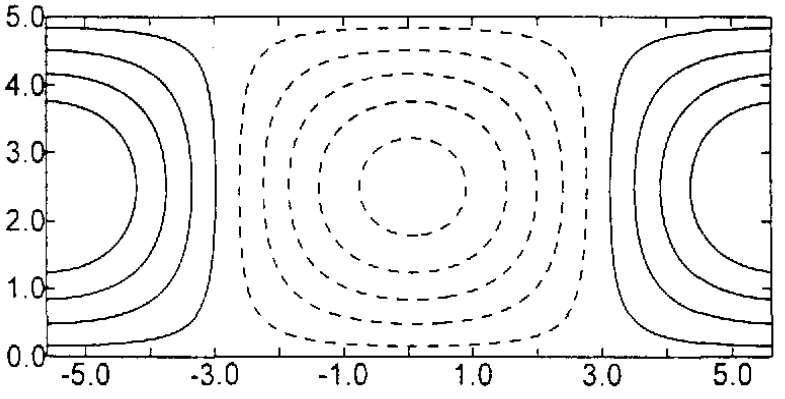

Fig. 3. The horizontal distribution of wavenumber–two topography. CI = 0.2.

where M_0 and a represent the initial amplitudes of the incipient block, in which M_0 represents the dipole component of the initial block and a denotes its monopole component. a_0 is the amplitude of the synoptic–scale eddies while the other parameters in (9a–b) are the same as in Luo and Li (2000). It should be noted that different incipient blocks can be constructed by choosing different values of both M_0 and a.

Without the loss of generality, we choose the parameters $M_0 = 0.45$, $a = 0.3$, $h_0 = 0.5$, $a_0 = 0.15 / \varepsilon$, $\gamma = 1.6$, $x_0 = 2.87 / 2$, and $\varepsilon = 0.24$ in our numerical experiment. We discuss three cases: the first focuses on the topography effect without synoptic–scale eddies ($h_0 = 0.5$ and $a_0 = 0$); the second focuses on synoptic–scale eddies without the topography effect ($h_0 = 0$ and $a_0 = 0.15 / \varepsilon$), and the third includes both the topography effect and synoptic–scale eddies ($h_0 = 0.5$ and $a_0 = 0.15 / \varepsilon$).

Case 1: Topography effect

Here, we discuss the interaction between an incipient block and a wavenumber–two topography. For the parameters $h_0 = 0.5$ and $a_0 = 0$, the wavenumber–two topography is shown in Fig. 3, while the streamfunction field (ψ) of the evolution of an incipient block interacting with a wavenumber–two topography is shown in Fig. 4.

Figure 3 shows the horizontal distribution of wavenumber–two topography at 55°N. The dashed region represents the ocean and the solid regions represent the continents. Figure 4 shows a planetary–scale blocking ridge over the topographic trough. This ridge appears to be in a phase–locking state and is not amplified into a typical blocking circulation during the time period considered. However, it can evolve into a blocking flow after a very long time. At the same time, weak synoptic–scale eddies are also induced by the topography effect (figures omitted). Perhaps, the weak synoptic–scale eddies play a certain role in the onset of blocking.

Case 2: Forcing of synoptic–scale eddies

In this subsection, we only discuss the interaction between an incipient block and synoptic–scale eddies. For $a_0 = 0.15 / \varepsilon$, during the interaction between an incipient block and synoptic–scale eddies, the planetary–scale field ($\psi \approx -\bar{u}y + \psi_p$) that consists of zonal wavenumbers 0–3, the synoptic–scale field (ψ_S) whick consists of zonal wavenumbers 7–25, and the total field ($\Psi_T = \psi + \psi_S$) are shown in Fig. 5.

It is shown in Fig. 5a that at day 0, this incipient block exhibits a weak blocking ridge (high–index flow). At the same time, the synoptic–scale eddies are located upstream of the

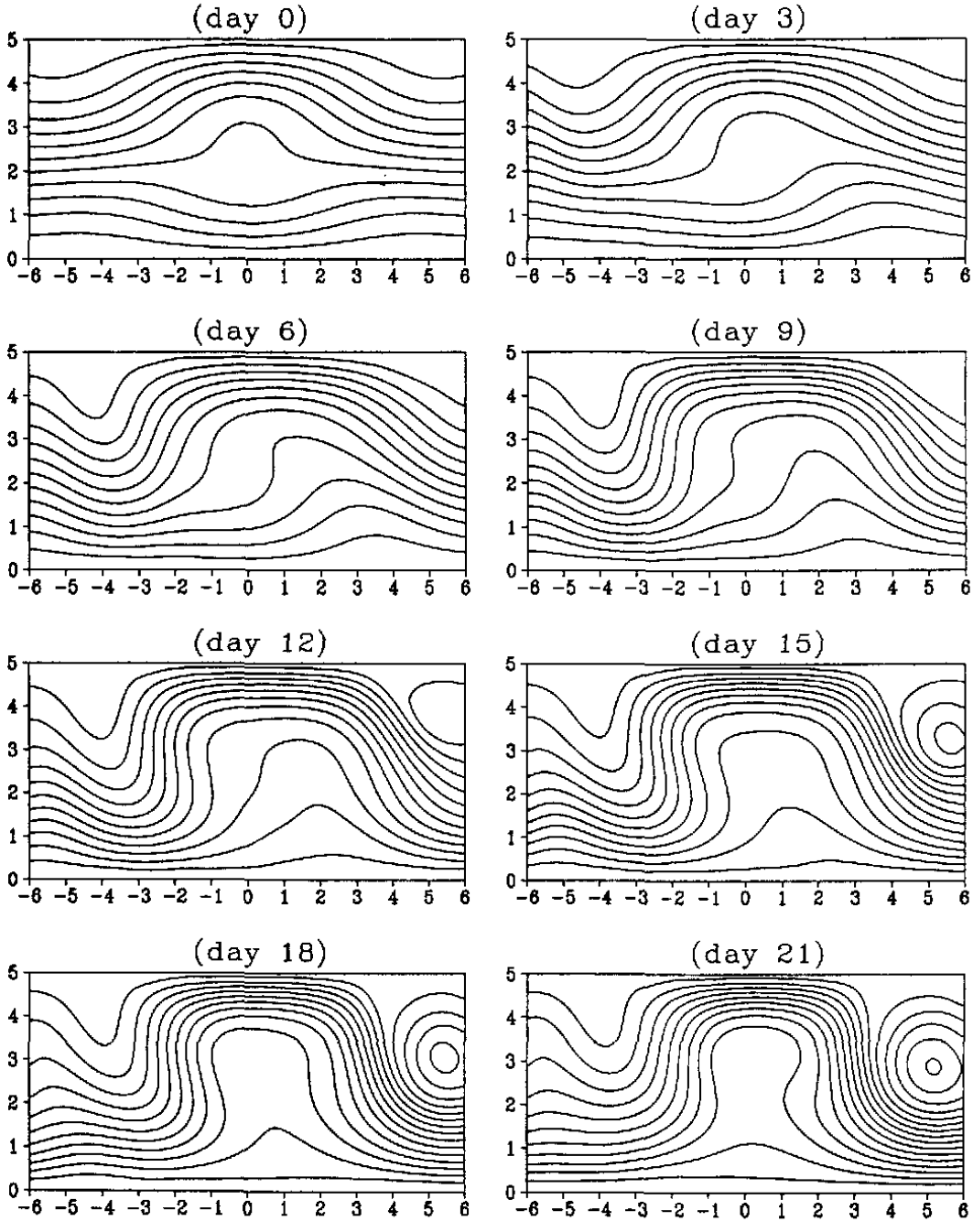

Fig. 4. The interaction of an incipient block with wavenumber–two topography for the parameters $M_0 = 0.45$ and $h_0 = 0.5$. CI = 0.232.

incipient block (Fig. 5b). The eddies will strengthen the incipient block downstream and create a blocking flow because their anticyclonic and cyclonic vortices enter into the block anticyclonic and cyclonic regions continuously. For example, at day 3 a very strong dipole block is excited and continues to strengthen. It seems to reach a maximum amplitude at day 6. After day 9 it begins to weaken so that a blocking high circulation can only be observed during the period between days 12 and 15. It almost disappears completely at day 21. Inspection

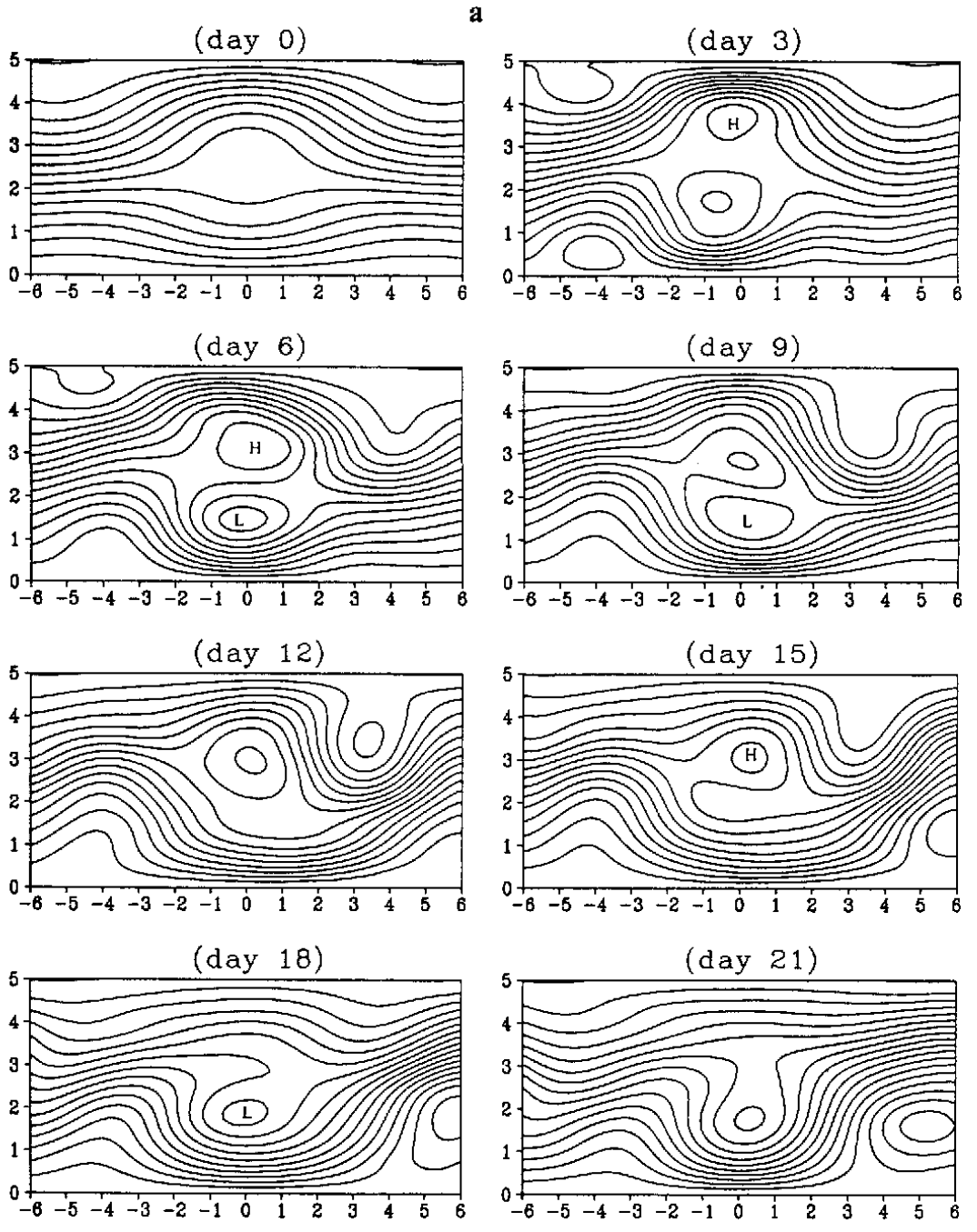

Fig. 5. The interaction of an incipient block with synoptic–scale eddies for the parameters $M_0 = 0.45$, $a = 0.3$, $h_0 = 0$, $a_0 = 0.15/\varepsilon$, $\gamma = 1.6$, $x_0 = 2.87/2$ and $\varepsilon = 0.24$. (a) Planetary–scale field, CI = 0.232; (b) synoptic–scale field, CI = 0.15; (c) total field, CI = 0.3.

of Fig. 5b indicates that the synoptic–scale eddies are split into two branches around the blocking region during the mature stage of blocking. This result compares rather well with observational evidences presented by Nakamura and Wallace (1990,1993). Unfortunately, in the total process the eddies are not enhanced by the feedback of the developing block. This point is not consistent with the observational aspects noted here. This may be caused by the

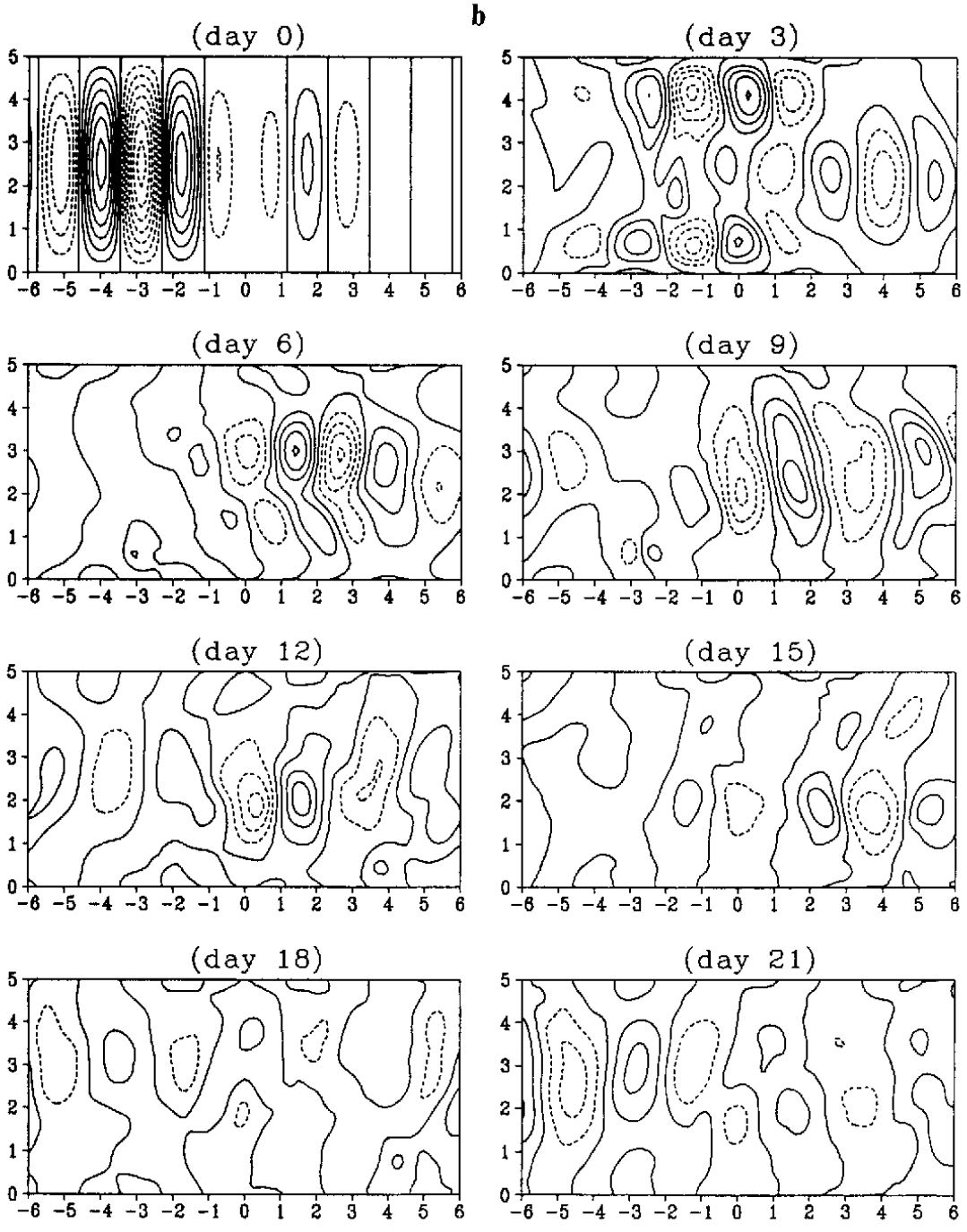

Fig. 5. (Continued).

lack of the continuous vorticity source that artificially causes synoptic–scale eddies (Shutts 1983; Haines and Holland 1998). Inspecting the total field in Fig. 5c, we find that the block flow by the synoptic–scale eddies seems to be comprised of several anticyclonic or cyclonic vortices. This block type was first found by Berggren et al. (1949) and then investigated by Nakamura and Wallace (1990, 1993), and is called "Berggren–type block" here. More recently, in a two–layer model, Luo (2000) proposed a transient–forced envelope soliton theory to successfully explain such a blocking structure. Unfortunately, that model cannot separate the

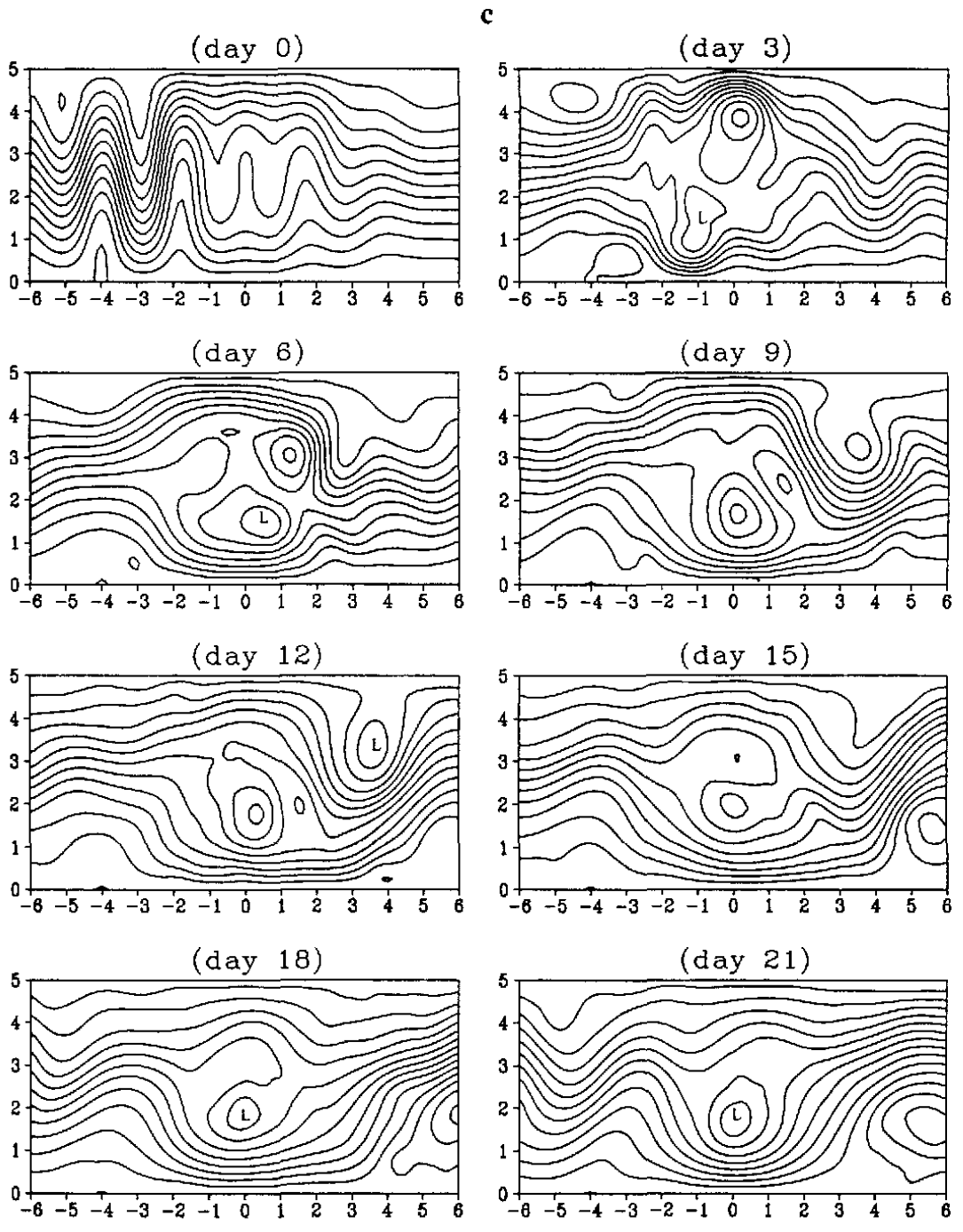

Fig. 5. (Continued).

different roles of synoptic–scale eddies and the topography effect in causing the blocking because of the lack of the topography effect. The present model, however, includes the topography effect, so it is able to discern the different roles of synoptic–scale eddies and the topography effect. Of course in producing blocking, large–scale heating should be added to the model. However, as the first step, this task is acceptable.

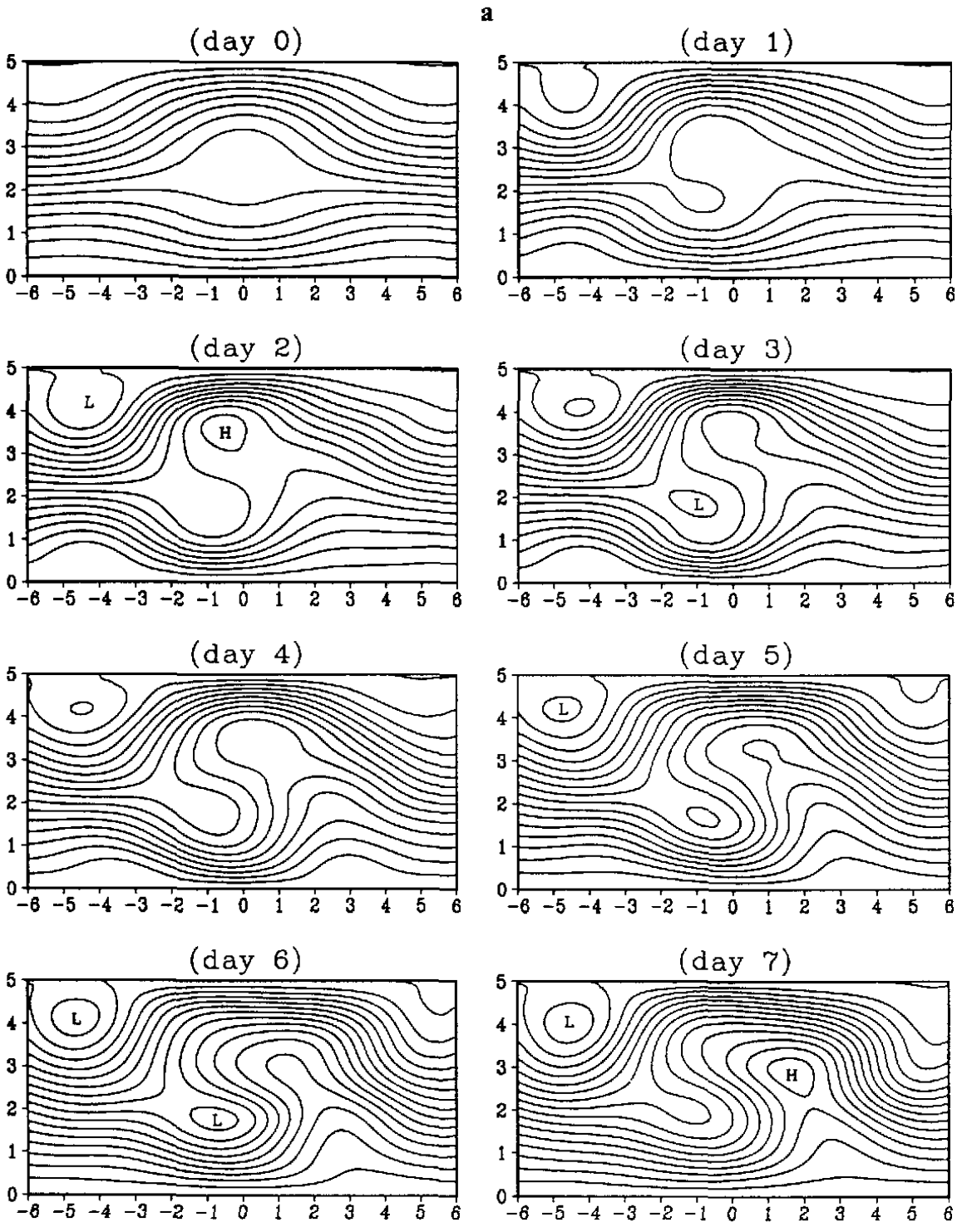

Fig. 6. The interaction of an incipient block with synoptic–scale eddies over a wavenumber–two topography for the parameters $M_0 = 0.45$, $a = 0.3$, $h_0 = 0.5$, $a_0 = 0.15/\varepsilon$, $\gamma = 1.6$, $x_0 = 2.87/2$ and $\varepsilon = 0.24$. (a) Planetary–scale field, CI = 0.232; (b) synoptic–scale field, CI = 0.15; (c) total field. CI = 0.3.

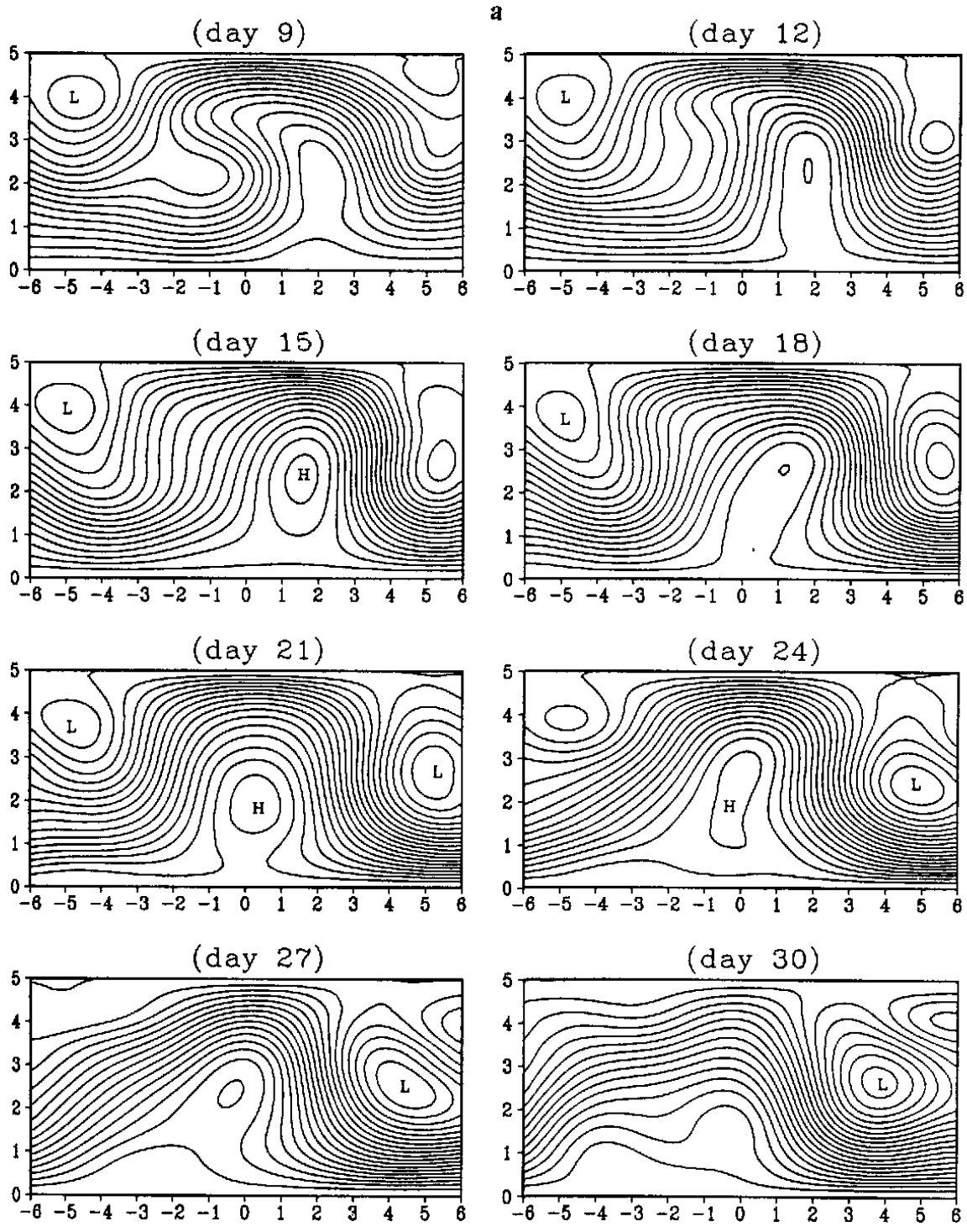

Fig. 6. (Continued).

Case 3: Joint forcing of synoptic–scale eddies and the topography effect

Here we will discuss the interaction of an incipient block with synoptic–scale eddies over a wavenumber–two topography. For $h_0 = 0.5$ and $a_0 = 0.15 / \varepsilon$, the planetary–scale field (ψ), the synoptic–scale field (ψ_S), and the total field (Ψ_T) are shown in Fig. 6.

Figure 6a seems to show the two life cycles of blocking. Before day 9, a dipole block is

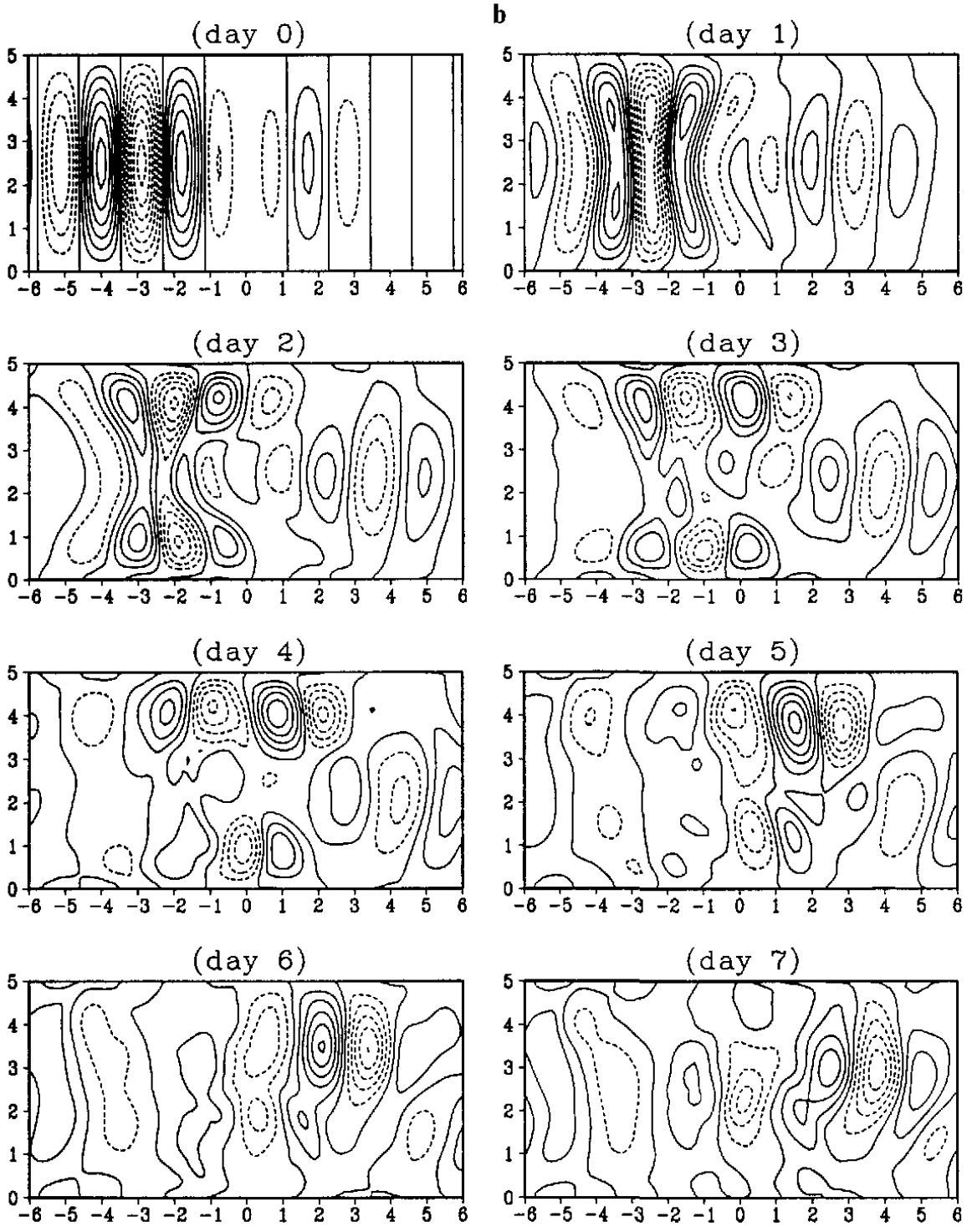

Fig. 6. (Continued).

formed and exhibits an asymmetric dipole structure. This dipole block looks similar in form to the first event (the period between 1 and 12 February 1989) of the Pacific blocks observed, in Fig. 1b. After day 9, the block flow exhibits an omega–type blocking high till day 27, which is also similar to the second event (the period between 14 and 21 February 1989) of the Pacific blocks. Thus, we can conclude that when both synoptic–scale eddies and the topography

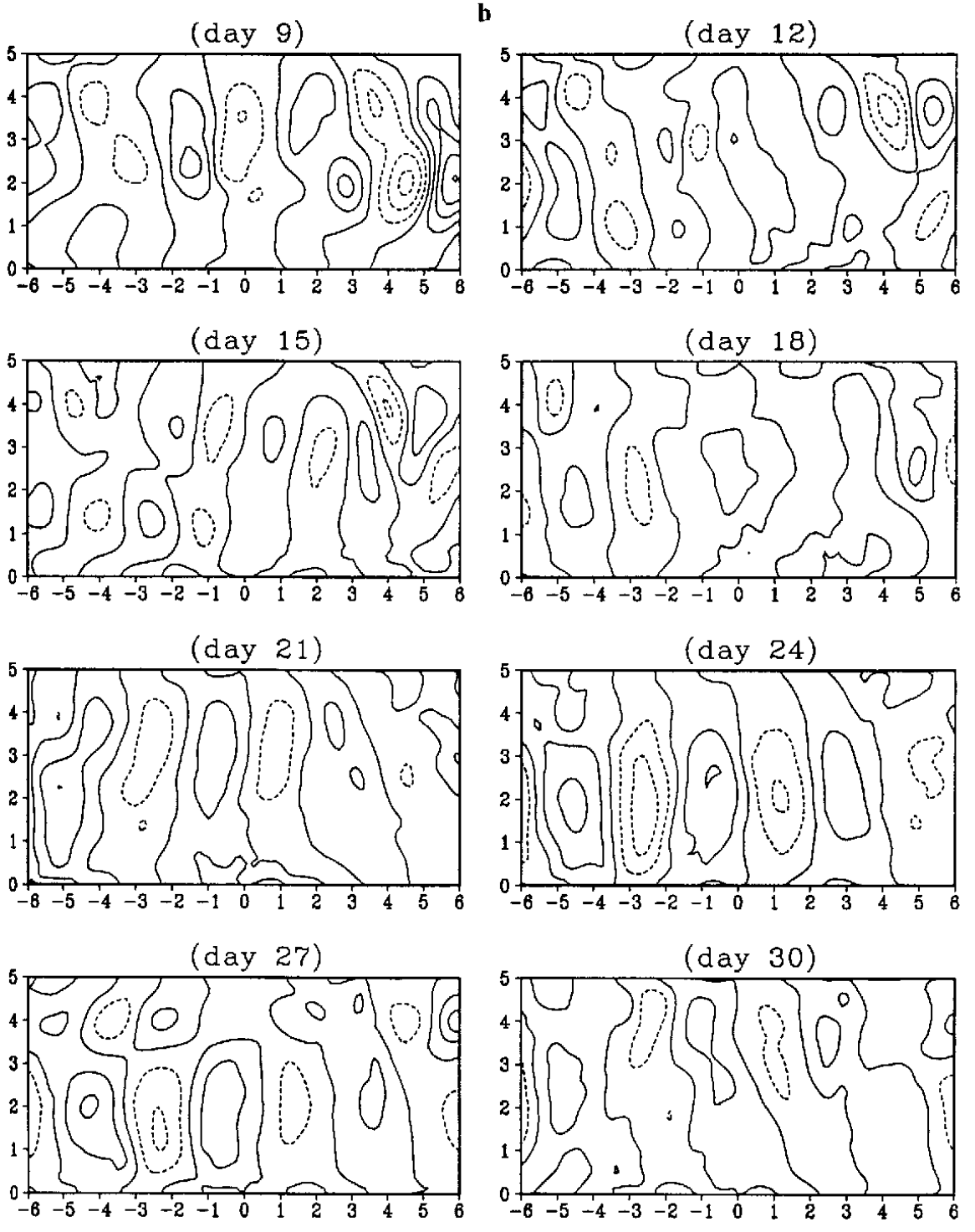

Fig. 6. (Continued).

effect are included, our numerical model can capture the main characteristics of the life cycle of real observed blocking events. Of course, there is a small discrepancy between observations and the results of the numerical model. In particular, the total field (Fig. 6c), looks very similar in form to that in Fig. 1a. On the other hand, we find that during the life cycle of blocking, the change of synoptic–scale eddies in our numerical model is also similar to the behavior of

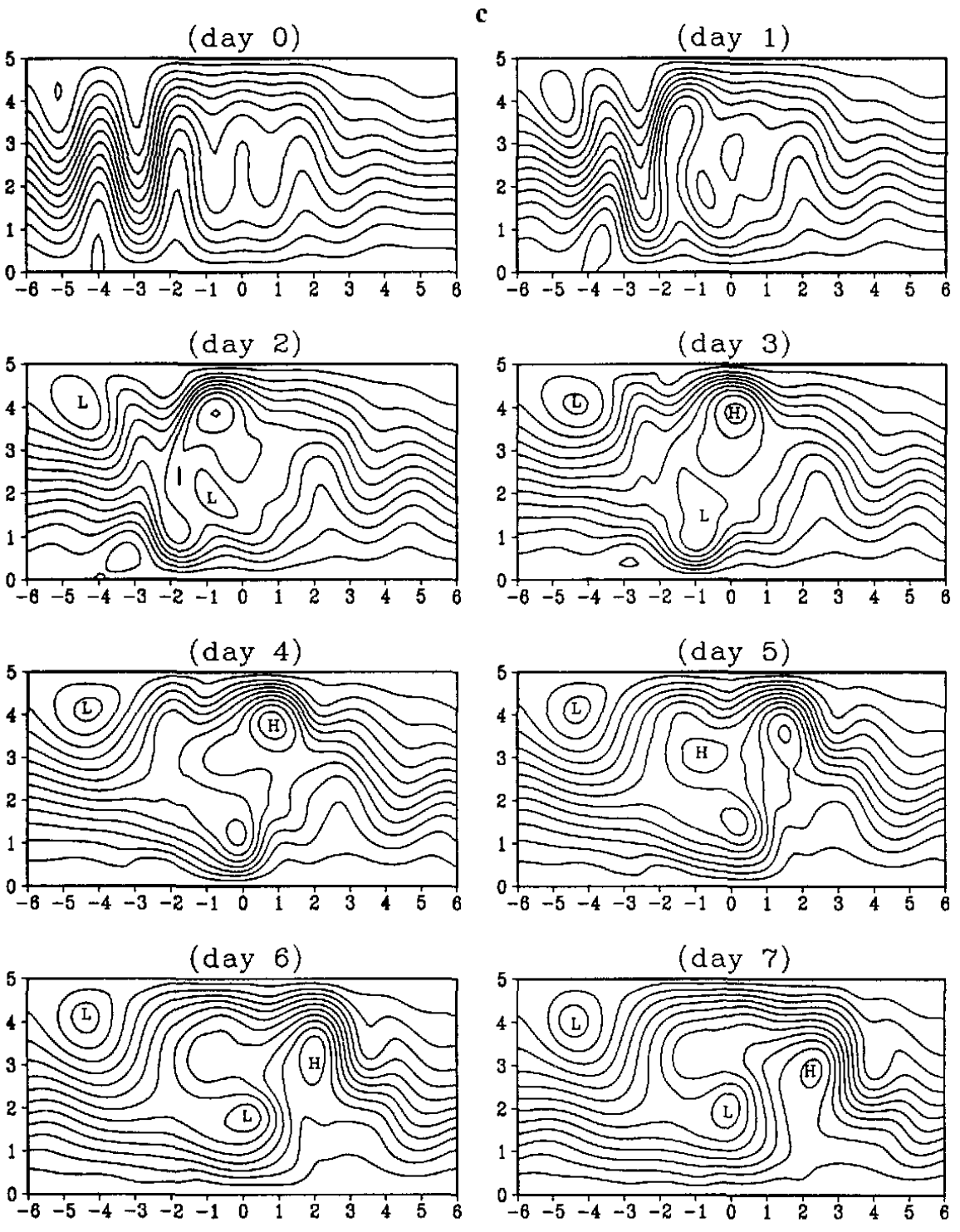

Fig. 6. (Continued).

observed synoptic–scale eddies in Fig. 1c. But the model is unable to reproduce the enhancement of synoptic–scale eddies before a blocking circulation is fully established (Nakamura and Wallace 1990, 1993). As pointed out above, the lack of the change in background westerly wind in the model may be a main reason for its failure in modelling the enhancement of synoptic–scale eddies during the blocking onset.

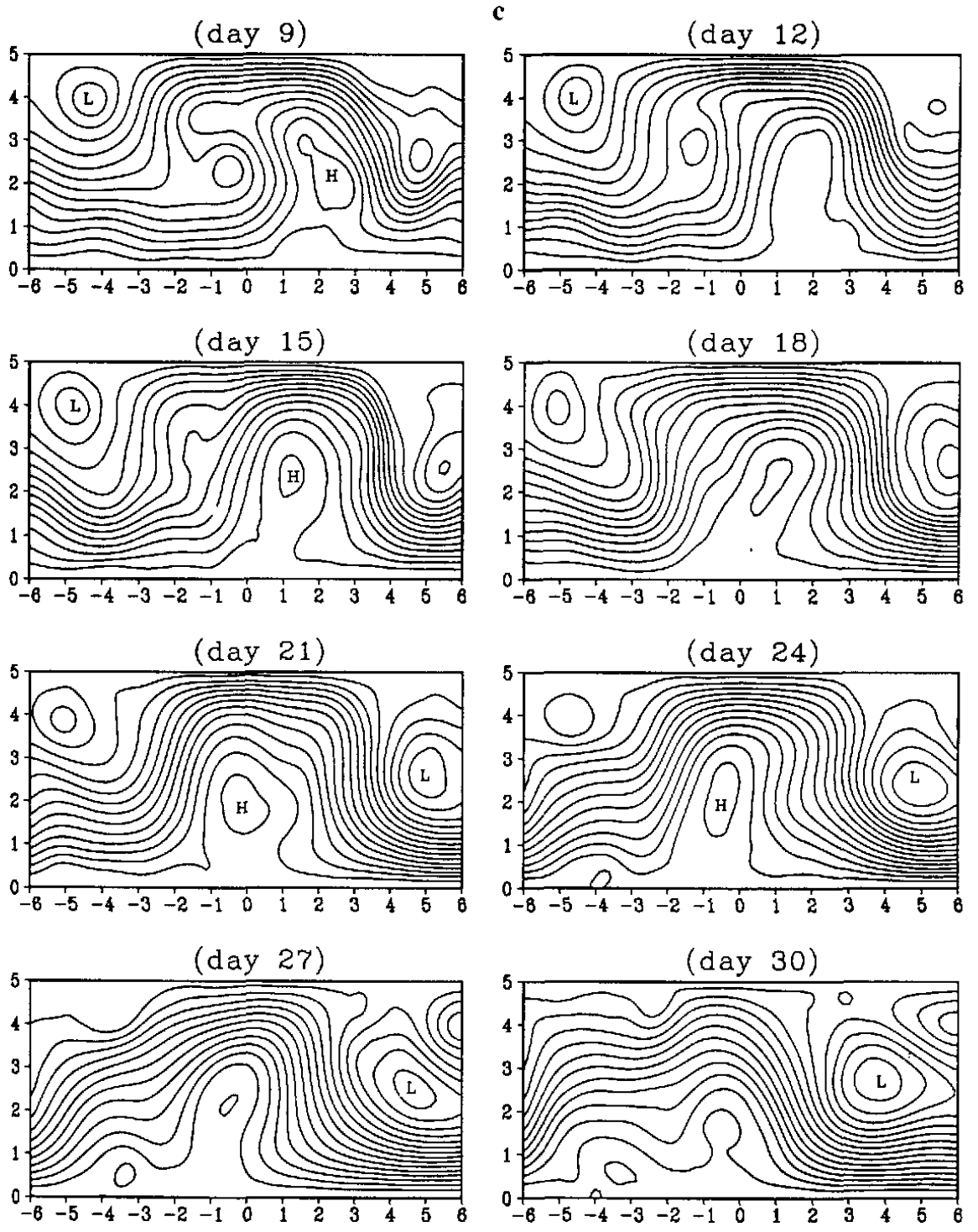

Fig. 6. (Continued).

As has been shown by Luo (1999, 2000) theoretically, the amplification of the dipole component of blocking is strongly associated with the resonant forcing of synoptic–scale eddies. This process may explain blocking events that are associated with cyclone waves. It can be concluded that the first blocking event observed during the period between 1 and 12 February 1989 might be completely excited by the synoptic–scale eddies, while the second block-

ing cycle might be associated with the topography effect. In the numerical model, the role of the topography effect in the life cycle of blocking can be reflected in part. However, in any case the synoptic–scale eddies seem to be more important for blocking onset than the topography effect, even though the latter plays a phase–locking role.

Another important result in this numerical experiment is that in the absence of the topography effect, the role of the synoptic–scale eddies seems to excite the dipole block, but in the presence of the topography effect the life period of the dipole block becomes particularly short, and the blocking high circulation seems to be dominant. Thus, the results obtained may explain, to some extent, why dipole blocks prevail over the Northern Atlantic and blocking high circulation prevails over the Northern Pacific.

4. Conclusions

In the present paper, a diagnostic study is made to verify that the life cycle of observed blocking exhibits a transfer between strong and weak dispersion (even non–dispersion). It is suggested that the instantaneous blocking flows observed over weather maps could be better represented by a transient–forced envelope Rossby soliton studied previously (Luo 1999, 2000; Luo et al. 2001). The mechanism of the formation, maintenance and decay of dipole blocking by synoptic–scale eddies can be better explained using the results from the eddy–forced envelope Rossby soliton theory.

The numerical experiments conducted indicate that the synoptic–scale eddies play a dominant role in the amplification of blocking compared to the topography effect, even though the latter may play a phase–locking role. These eddies tend to split into two branches around the blocking region during the onset of blocking.

On the other hand, the lack of the forcing of large–scale diabatic heating and realistic topography may also affect the numerical results. This remains to be quantified. However, inclusion of these factors may further improve our understanding of the mechanism of blocking if the role of pure synoptic–scale eddies in the onset, maintenance and decay of blocking can be clarified. These problems derseve further study.

Acknowledgments. This research was supported by the TRAPOYT and by the National Natural Science Foundation of China under Grant No. 40023001.

REFERENCES

Berggren, R., B. Bolin, and C. G. Rossby, 1949: An aerological study of zonal motion, its perturbations and break–down. *Tellus*, **2**, 14–37.

Charney, J. G., and J. G. DeVore, 1979: Multiple flow equilibria in the atmosphere and blocking. *J. Atmos. Sci.*, **35**, 1205–1216.

Chen, W. Y., and H. H. Juang, 1992: Effects of transient eddies on blocking flows: General circulation model experiments. *Mon. Wea. Rev.*, **120**, 787–801.

Colucci, S. J., 1985: Explosive cyclogenesis and large–scale circulation changes: Implications for atmospheric blocking. *J. Atmos. Sci.*, **42**, 2701–2717.

Colucci, S. J., 1987: Comparative diagnosis of blocking versus nonblocking planetary–scale circulation changes during synoptic–scale cyclogenesis. *J. Atmos. Sci.*, **44**, 124–139.

Egger, J., 1978: Dynamics of blocking highs. *J. Atmos. Sci.*, **35**, 1788–1801.

Egger, J., Metz, W., and G. Müller, 1986: Synoptic–scale eddy forcing of planetary–scale blocking anticyclones. *Adv. Geophys.*, **29**.

Ek, N. R., and G. E. Swaters, 1994: Geostrophic scatter diagrams and the application of quasi-geostrophic free mode theory to a northeast Pacific blocking episode. *J. Atmos. Sci.*, **51**, 563–581.

Green, J. S. A., 1977: The weather during July 1977: Some dynamical considerations of the drought. *Weather*, **32**, 120–126.

Hansen, A., and T. C. Chen, 1982: A spectral energetics analysis of atmospheric blocking. *Mon. Wea. Rev.*, **110**, 1146–1159.

Haines, K., and A. J. Holland, 1998: Vacillation cycles and blocking in a channel. *Quart. J. Roy. Meteor. Soc.*, **124**, 873–895.

Haines, K., and J. C. Marshall, 1987: Eddy-forced coherent structures as a prototype of atmospheric blocking. *Quart. J. Roy. Meteor. Soc.*, **113**, 681–704.

Holopainen, E., and C. Fortelius, 1987: High-frequency transient eddies and blocking. *J. Atmos. Sci.*, **44**, 1632–1645.

Illari, L., and J. C. Marshall, 1983: On the interpretation of eddy fluxes during a blocking episode. *J. Atmos. Sci.*, **40**, 2232–2242.

Illari, L., 1984: A diagnostic study of the potential vorticity in a warm blocking anticyclone. *J. Atmos. Sci.*, **41**, 3518–3526.

Ji, L. R., and L. Tibaldi, 1983: Numerical simulations of a case of blocking. The effects of orography and land-sea contrast. *Mon. Wea. Rev.*, **111**, 2068–2086.

Lupo, A. R., and P. J. Smith, 1995: Planetary and synoptic-scale interactions during the life cycle of a mid-latitude blocking anticyclone over the North Atlantic. *Tellus*, **47A**, 575–596.

Luo, D., 1999: *Large-scale Envelope Rossby Soliton Theory in the Atmosphere and Blocking Circulations*, China Meteorological Press.

Luo, D., 2000: Planetary-scale baroclinic envelope Rossby solitons in a two-layer model and their interaction with synoptic-scale eddies. *Dyn. Atmos. Oceans*, **32**, 27–74.

Luo D., and Li, J., 2000: Barotropic interaction between planetary- and synoptic-scale waves during the life cycles of blockings. *Advances in Atmospheric Sciences*, **17**, 649–670.

Luo, D., F. Huang, and Y. Diao, 2001: Interaction between planetary-scale envelope soliton blocking anticyclones and synoptic-scale eddies: Observations and theory. *J. Geophys. Res.*, **106**, D 23, 31795–31815.

Malanotte-Rizzoli, P., and P. Malguzzi, 1987: Coherent structures in a baroclinic atmosphere. Part III: Block formation and eddy forcing. *J. Atmos. Sci.*, **44**, 2493–2505.

Malguzzi, P., and P. Malanotte-Rizzoli, 1984: Nonlinear stationary Rossby waves on nonuniform zonal winds and atmospheric blocking. Part I: The analytical theory. *J. Atmos. Sci.*, **41**, 2620–2628.

Malguzzi, P., 1993: An analytical study on the feedback between large- and small-scale eddies. *J. Atmos. Sci.*, **50**, 1429–1436.

McWilliams, J. C., 1980: An application of equivalent modons to atmospheric blocking. *Dyn. Atmos. Oceans*, **5**, 219–238.

Metz, W., 1986: Transient cyclone-scale vorticity forcing of blocking highs. *J. Atmos. Sci.*, **43**, 1467–1483.

Mullen, S. L., 1987: Transient eddy forcing of blocking flows. *J. Atmos. Sci.*, **44**, 3–22.

Nakamura, H., and J. M. Wallace, 1990: Observed changes in baroclinic wave activity during the life cycles of low-frequency circulation anomalies. *J. Atmos. Sci.*, **47**, 1100–1116.

Nakamura, H., and J. M. Wallace, 1993: Synoptic behavior of baroclinic eddies during the blocking onset. *Mon. Wea. Rev.*, **121**, 1892–1903.

Nakamura, H., M. Nakamura, and J. L. Anderson, 1997: The role of high- and low-frequency dynamics in blocking formation. *Mon. Wea. Rev.*, **125**, 2074–2093.

Reinhold, B. B., and R. T. Pierrehumbert, 1982: Dynamics of weather regimes: quasi- stationary waves and blocking. *Mon. Wea. Rev.*, **110**, 1105–1145.

Shutts, G. J., 1983: The propagation of eddies in diffluent jetstreams: eddy vorticity forcing of blocking flow fields. *Quart. J. Roy. Meteor. Soc.*, **109**, 737–761.

Shutts, G. J., 1986: A case study of eddy forcing during an Atlantic blocking episode. *Advances in Geophysics*, Academic Press, **29**, 135–162.

Tanaka, H. L., 1991: A numerical simulation of amplification of low frequency planetary waves and blocking formations by the upscale energy cascade. *Mon. Wea. Rev.*, **119**, 2919–2935.

Tsou, C. S., and Smith, P. J., 1990: The role of synoptic / planetary-scale interactions during the development of a blocking anticyclone. *Tellus*, **42A**, 174–193.

Vautard, R., B. Legras, and M. Déqué, 1988: On the source of midlatitude low-frequency variability. Part I: A statistical approach to persistence. *J. Atmos. Sci.*, **45**, 2811–2844.

Vautard, R., and B. Legras, 1988: On the source of midlatitude low-frequency variability. Part II: Nonlinear equilibration of weather regimes. *J. Atmos. Sci.*, **45**, 2845–2867.

Yeh, T. C., 1949: On energy dispersion in the atmosphere. *J. Meteorol.*, **6**, 1–16.

天气尺度波激发的阻塞流的生命循环: 观测结果和数值试验

罗德海 李建平 黄 菲

摘 要

通过观测研究证实了天气尺度波激发的阻塞流的生命循环是频散和非频散之间的转换过程。除此之外，进行了一个数值试验，发现天气尺度波似乎对阻塞的形成起支配作用，而地形似乎起位相锁相的作用。同时可以发现天气尺度波在阻塞的产生过程中分裂成两支。这些结果支持了我们所得到的观测结果。

关键词: 阻塞, 生命周期, 天气尺度涡